JOURNAL OF PHYSICAL ORGANIC CHEMISTRY, VOL. 8, 473–483 (1995)

THEORETICAL STUDIES OF THE IDENTITY ALLYL TRANSFER REACTIONS*

IKCHOON LEE,† CHANG KON KIM AND BON-SU LEE
Department of Chemistry, Inha University, Inchon 402-751, Korea

Ab initio studies on the S_N2 identity exchange reactions $RCH_2X + X^- \rightarrow X^- + RCH_2X$ for $R = CH_2CH$ with $X^- = H$, NH_2, OH, F, PH_2, SH and Cl, and for $R = CH_3$ and $CH{\equiv}C$ with $X^- = Cl$ were carried out at the HF and MP2 levels using the 6-31++G basis sets. The activation barriers, $\Delta E^{\neq}$, and major structural changes, $\Delta d^{\neq}(C\text{–}X)$, in the activation process are closely related to the electronegativity of the R and X groups. The effect of electronegativity is twofold: a stronger electronegativity of R and/or X leads to a lesser electronic as well as structural reorganization required in the activation and to a greater correlation energy in the transition state. The former effect lowers the energy barriers at both the HF and MP2 levels whereas the latter lowers only the correlated (MP2) activation energies. Results with $R = CH_2CH$, as a model for $R = C_6H_5$, indicate that 'benzylic effect' arises mainly from the relatively stronger electron acceptor ability of the phenyl group.**

INTRODUCTION

Bimolecular nucleophilic substitution reactions at carbon have been extensively studied experimentally and theoretically. Recently, much work has focused on the gas-phase reactions in order to clarify intrinsic features of S_N2 processes. In this respect, gas-phase identity exchange reactions, in which the nucleophile and leaving group are the same, have attracted considerable attention from experimentalists[2] and theoreticians.[3]

Theoretical studies of gas-phase identity exchange reactions have played an essential role in providing evidence for a double-well potential energy surface (PES) and in establishing usefulness of the Marcus equation[4] by showing remarkably good agreement between intrinsic barriers calculated MO theoretically and those derived from the Marcus equation.[3a–c,3i]

Most of these theoretical studies have, however, involved methyl transfer reactions, R = H in the equation (1)

$$X^- + RCH_2X \rightleftharpoons XCH_2R + X^- \qquad (1)$$

In a series of theoretical studies on methyl transfer reactions, Shi and Boyd[3h,i] stressed the importance of including diffuse functions in the basis set and incorporating electron correlation effects in the calculation. They showed that the intrinsic barrier is related to the electronegativity of the leaving group, X^-; as the electronegativity of the leaving group increases, the intrinsic barrier decreases. Recently, Wladkowski *et al.*[3j] reported a comprehensive study on the S_N2 identity exchange reaction involving acetonitrile group transfer, R = CN in equation (1). They concluded that the effect of CN substitution on the stability of the S_N2 transition state (TS) does not arise from 'resonance' effects in the TS.

Delocalization of π or lone-pair electrons of the nucleophile into the substrate benzene ring in the S_N2 reactions of the benzyl derivatives is known to stabilize the TS, I, and results in a rate enhancement.[5] This 'benzylic effect' causes bond contraction of the C^{α}–C^{β} bond.

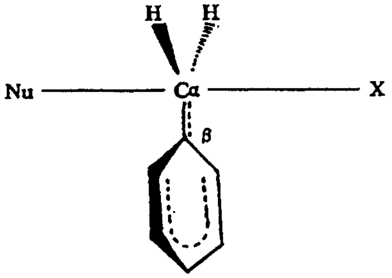

I

To extend our understanding of the factors that are important in controlling the intrinsic reactivities, we have carried out *ab initio* MO calculations on the identity allyl transfer reactions, $R = CH_2CH$ in equation (1), with X = H,

---

[*] Determination of Reactivity by MO Theory, Part 85. For Part 84, see Ref. 1.

[†] Author for correspondence.

CCC 0894–3230/95/070473–11

Received 20 December 1994
Revised 10 March 1995

NH_2, OH, F, PH_2, SH and Cl. We have also investigated the effect of α-substitution on the reactivity by including $R = CH_3$ and $HC{\equiv}C$ in equation (1) for X = Cl.

COMPUTATIONAL METHOD

The 6–31G extended basis sets with diffuse functions and polarization functions (6–31++G**)[7] were used throughout. To account for the electron correlation, second-order Møller–Plesset perturbation theory (MP2) was adopted. The MP2 calculations are known to give size-consistent results, which is an important requirement for the study of chemical reactivity. We kept the same level of computation in the energy calculation as that used in geometry optimization. Unless noted otherwise, two types of results are reported: HF (HF/6–31++G**//HF/6–31++G**) and MP2 (MP2/6–31++G**//MP2/6–31++G**).[7] In order to examine the effects of diffuse and polarization functions on the calculated geometries, 6–31+G* (and 6–31++G*) level[7] computations were also performed for X = H, F and Cl.

Geometries were optimized using analytical energy gradient methods at the HF and MP2 levels. The geometries of reactants and TSs were fully optimized with C_s symmetry constraint for the latter, and all positive and only one negative eigenvalues, respectively, in the Hessian matrix were identified to confirm the equilibrium and transition states[8] in all the HF level calculations. For X = F, an additional very low negative frequency (57·0i cm^{-1}) was obtained but this was found to reduce further at the MP2 level (24·9i cm^{-1}). The transition vector for this low imaginary frequency was found to correspond to a weak bending mode. As Wu and Houk[9] have pointed out, low imaginary frequencies can occur due to bending in addition to rotation on very flat potential surfaces. (We have calculated the TS structure under C_1 symmetry constraint with full geometry optimization and arrived at a structure in which $C^1C^2C^3F_2$ heavy atoms are coplanar with two hydrogens on C^3 perpendicular to this plane. This TS structure had only one negative eigenvalue (640·5i cm^{-1}), 1·8 kcal mol^{-1} lower at the HF level but higher by 0·3 kcal mol^{-1} at the MP2 level than the energies at the corresponding levels under C_s symmetry constraint, indicating that the potential is very flat around the TS.) Population analyses were performed by natural bond orbitals (NBO) method.[10] Geometries of reactant (ion–molecule) complexes corresponding to backside attack were fully optimized. All calculations were carried out using the Gaussian 90 and 92 program.[11]

RESULTS AND DISCUSSION

Geometries

Optimized geometries of substrates (S), ion–molecule complexes (C) and transition states (TS) at the HF and MP2 levels are summarized in Table 1. The data reveal that in general the HF results give shorter bond distances in the substrate molecule than the MP2 results. For X = H, however, both the HF and MP2 results give bond lengths which are very close to the experimental results (within ±0·003 Å), except for $d(C^1–C^2)$[12] [experimental bond lengths are $d(C^1 0 C^2) = 1·318$ and $d(C^2 0 C^3) = 1·501$ Å]; the MP2 level overestimates this length by 0·02 Å. In all cases, bond length changes along reaction coordinate (S → C → TS) are significant for $d(C^2–C^3)$, $d(C^3–X^{6,7})$ and $d(C^3–H^{4,5})$; $d(C^3–H^{4,5})$ is lengthened in the ion–molecule complex whereas it is shortened again in the TS. The important bond length changes are, however, those of $d(C^2–C^3)$ and $d(C^3–X^{6,7})$ involved in the activation, i.e. $\Delta d^{\ne}$(S→TS) values. The basis set dependence of these two bond lengths is summarized in Table 2 for X = H, F and Cl. Examination of Table 2 indicates that the most significant structural change in the activation process is the extension of C^3–X since the decrease in the C^2–C^3 distance [$\Delta d^{\ne}(C^2–C^3)$] is very small compared with the increase in the C^3–X^6 distance [$\Delta d^{\ne}(C^3–X^6)$]. The extension of the double bond, $\Delta d^{\ne}(C^1–C^2)$, is less than 1% in all cases and hence is negligible. Inclusion of electron correlation generally shortens further the distances of the two bonds. Additions of polarization and diffuse functions lead very small changes in the HF level bond lengths. By far the greater changes are accompanied by inclusion of the electron correlation effect; nearly a 10% bond length decrease is effected by the inclusion of electron correlation with the 6–31++G** basis set. For heavy-atom Xs (X = F and Cl), the percentage changes in $\Delta d^{\ne}(C^3–X^6)$ value are smaller than those for X = H and also the effects of adding polarization and diffuse functions in addition to including electron correlation are much smaller than those for X = H.

The angle $a(C^1C^2C^3)$ deviates slightly from 120° in all three structures, S, C and TS, with the MP2 result giving the nearest value to 120°. Angles $a(C^2C^3X^6)$ and $D(C^1C^2C^3X^6)$ approach 90° at the TS, but here again the MP2 values are the nearest to 90°. Since a C_s symmetry constraint is applied to the TS, the angle $D(C^1C^2C^3H^4)$ is 0°.

Energy barriers

Two types of energy barriers, the activation energy, $\Delta E^{\ne}$, and the intrinsic barrier, $E_0^{\ne}$, in Figure 1, were determined and summarized in Table 3. We note that inclusion of electron correlation tends to reduce both the activation barrier and the intrinsic barrier. The energy barriers, $\Delta E^{\ne}$ and $E_0^{\ne}$, for the identity exchange reactions separate into three groups depending on the row of the Periodic Table; X = H alone belongs to the first group, X = NH_2, OH and F to the second and X = PH_2, SH and Cl to the third. Similar classification of X into separate groups were reported for the $\Delta E_0^{\ne}$

Table 1. Optimized geometries of substrates (S), ion–molecule complexes (C) and transition state (TS) at the HF and MP2 levels

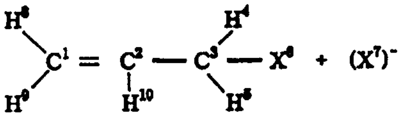

			Bond lengths (Å)			Bond angles (°)		Dihedral angles (°)	
X	Species	Level	$d(C^2–C^3)$	$d(C^3–X^6)$	$d(C^3–H^4)$	$a(C^2C^3X^6)$	$a(C^2C^3)H^4)$	$D(C^1C^2C^3X^6)$	$D(C^1C^2C^3H^4)$
H	S	HF	1·5025	1·0869	1·0845	110·76	111·42	120·62	0·00
		MP2	1·4989	1·0914	1·0899	110·99	110·93	120·46	0·00
	C	HF	1·5002	1·0858	1·0876	109·95	111·96	121·63	0·05
		MP2	1·3982	1·0916	1·0930	110·20	111·81	121·46	0·07
	TS	HF	1·4811	1·6702	1·0630	92·31	121·12	91·88	0·00
		MP2	1·4781	1·5712	1·0741	89·98	121·36	91·30	0·00
NH_2	S	HF	1·5039	1·4578	1·0842	110·78	109·43	124·75	5·50
		MP2	1·4988	1·4710	1·0912	110·13	109·26	120·71	2·40
	C	HF	1·5069	1·4491	1·0838	111·81	109·65	131·09	10·92
		MP2	1·5001	1·4636	1·0912	111·62	109·60	123·58	4·33
	TS	HF	1·4767	2·0422	1·0632	92·07	119·86	94·20	0·00
		MP2	1·4638	2·0181	1·0783	91·11	119·59	94·11	0·00
OH	S	HF	1·4991	1·4066	1·0871	108·29	110·13	128·24	6·74
		MP2	1·4934	1·4369	1·0946	107·46	109·95	122·82	1·99
	C	HF	1·5114	1·4261	1·0814	111·26	111·12	186·57	48·62
		MP2	1·5051	1·4568	1·0888	111·14	111·32	191·36	42·82
	TS	HF	1·4779	1·9556	1·0611	92·41	119·79	91·31	0·00
		MP2	1·4661	1·9425	1·0736	91·36	119·65	90·75	0·00
F	S	HF	1·4959	1·3797	1·0819	109·64	111·68	125·53	6·21
		MP2	1·4903	1·4170	1·0899	109·45	111·57	120·80	2·27
	C	HF	1·4957	1·4052	1·0843	107·67	111·05	121·32	5·41
		MP2	1·4880	1·4447	1·0923	107·51	110·93	120·42	5·40
	TS	HF	1·4798	1·8605	1·0619	93·91	119·88	91·79	0·00
		MP2	1·4710	1·8467	1·0739	93·11	119·59	91·46	0·00
PH_2	S	HF	1·5029	1·8752	1·0797	111·64	110·18	110·11	−9·00
		MP2	1·4970	1·8759	1·0917	110·52	109·75	108·90	−9·80
	C	HF	1·5011	1·8725	1·0866	111·41	110·66	105·01	−14·38
		MP2	1·4933	1·8727	1·0934	109·92	110·52	106·44	−13·17
	TS	HF	1·4702	2·6079	1·0638	94·83	121·09	91·38	0·00
		MP2	1·4579	2·5099	1·0760	91·28	121·15	90·76	0·00
SH	S	HF	1·5007	1·8338	1·0814	109·61	110·71	115·76	−5·25
		MP2	1·4952	1·8314	1·0895	108·89	110·08	113·70	−7·37
	C	HF	1·4996	1·8347	1·0783	111·72	111·92	134·40	9·21
		MP2	1·4950	1·8309	1·0865	112·35	111·13	137·43	12·94
	TS	HF	1·4693	2·5349	1·0625	95·75	120·54	91·94	0·00
		MP2	1·4633	2·4111	1·0729	92·86	120·22	91·99	0·00
Cl	S	HF	1·4954	1·8045	1·0787	111·25	111·84	119·74	−0·50
		MP2	1·4902	1·7971	1·0878	111·15	110·92	117·62	−1·81
	C	HF	1·4928	1·8282	1·0782	110·15	112·11	112·57	−4·65
		MP2	1·4869	1·8123	1·0884	110·23	111·18	111·95	−5·89
	TS	HF	1·4618	2·4991	1·0642	98·89	120·59	92·43	0·00
		MP2	1·4604	2·3625	1·0733	96·05	120·00	92·65	0·00

values of identity methyl transfer reactions by Shi and Boyd.[3i] They attributed this grouping to the type of hybridization and the electronic structure of the TS. No doubt periodicity of homonuclear single covalent bond energies of the heavy-atom elements in X plays an important role for this grouping, since the bond energies of the two corresponding first- and second-row elements differ uniformly by *ca* 20 kcal mol^{-1} (1 kcal = 4·184 kJ).[12] Within each group, the $\Delta E^{\ddagger}$ and $\Delta E_0^{\ddagger}$ values, at both the HF and MP2 levels, vary linearly with electronegativity (χ) (the theoretical values are generally in good agreement with those for X

Table 2. Basis set dependence of bond lengths (Å)

X	Basis set	Species	d(C^1–C^2)	d(C^2–C^3)	d(C^3–X)
H	HF/6–31+G*	GS	1·3223	1·5029	1·0868
		TS	1·3277	1·4775	1·6898
		$\Delta d^{\ddagger}$	+0·0054	−0·0254 (−1·7)[a]	+0·6030 (+55·5)[a]
	MP2/6–31+G*	GS	1·3400	1·4989	1·0954
		TS	1·3461	1·4689	1·6367
		$\Delta d^{\ddagger}$	+0·0061	−0·0300 (−2·0)	+0·5413 (+49·4)
	HF/6–31++G**	GS	1·3222	1·5025	1·0869
		TS	1·3263	1·4811	1·6702
		$\Delta d^{\ddagger}$	+0·0041	−0·0214 (−1·4)	+0·5833 (+53·7)
	MP2/6–31+G**	GS	1·3396	1·4971	1·0902
		TS	1·3435	1·4763	1·5707
		$\Delta d^{\ddagger}$	+0·0039	−0·0208 (−1·4)	+0·4805 (+44·1)
F	HF/6–31+G*	GS	1·3208	1·4962	1·3789
		TS	1·3197	1·4802	1·8589
		$\Delta d^{\ddagger}$	−0·0011	−0·0160 (−1·1)	+0·4800 (+34·8)
	MP2/6–31+G*	GS	1·3398	1·4891	1·4178
		TS	1·3419	1·4699	1·8497
		$\Delta d^{\ddagger}$	+0·0021	−0·0192 (−1·3)	+0·4319 (+30·5)
	HF/6–31++G**	GS	1·3207	1·4959	1·3797
		TS	1·3196	1·4798	1·8605
		$\Delta d^{\ddagger}$	−0·0011	−0·0161 (−1·1)	+0·4808 (+34·8)
	MP2/6–31++G**	GS	1·3391	1·4886	1·4156
		TS	1·3412	1·4689	1·8457
		$\Delta d^{\ddagger}$	+0·0021	−0·0197 (−1·3)	+0·4301 (+30·4)
Cl	HF/6–31+G*	GS	1·3210	1·4957	1·8040
		TS	1·3214	1·4623	2·4966
		$\Delta d^{\ddagger}$	+0·0004	−0·0334 (−2·2)	+0·6926 (+38·4)
	HF/6–31++G**	GS	1·3208	1·4954	1·8045
		TS	1·3214	1·4618	2·4991
		$\Delta d^{\ddagger}$	+0·0006	−0·0336 (−2·3)	+0·6946 (+38·5)
	MP2/6–31++G**	GS	1·3391	1·4887	1·7-91-952
		TS	1·3430	1·4585	2·3600
		$\Delta d^{\ddagger}$	+0·0039	−0·0302 (−2·0)	+0·5648 (+31·5)

[a] Values in parentheses are percentage changes: $(\Delta d^{\ddagger}/d^0) \times 100$.

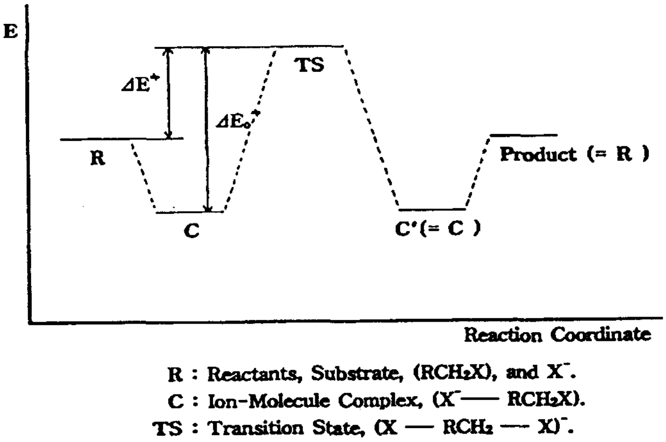

Figure 1. Two types of energy barriers, the activation energy, $\Delta E^{\ddagger}$, and the intrinsic barrier, $\Delta E_0^{\ddagger}$, of the gas-phase identity exchange reaction in equation (1)

Table 3. Energies (kcal mol^{-1}) calculated at the HF and MP2 levels for reactions $CH_2CHCH_2X + X^-$

	HF		MP2		
X	$\Delta E_0^{\ddagger}$	$\Delta E^{\ddagger a}$	$\Delta E_0^{\ddagger}$,	$\Delta E^{\ddagger}$	χ^b
H	67·07	61·83	55·13	49·90	–
NH_2	56·66	40·04	43·34	24·79	6·16
OH	(40·11)[c]	28·58	(27·88)[c]	14·66	6·95
F	22·96	8·82	14·98	−0·29	10·01
PH_2	44·87	38·63	33·26	22·54	5·05
SH	(30·11)[c]	23·52	(24·92)[c]	14·78	5·69
Cl	16·82	8·30	18·80	8·11	7·65

[a] Corrected for zero-point energies.
[b] Group electronegativities calculated at the CI(SD) level.[13]
[c] Ion–molecule complex energy under backside attacking constraint for X^-.

radicals[14]) of the X group (Figures 2 and 3). The activation barrier, $\Delta E^{\ddagger}$, and intrinsic barrier, $\Delta E_0^{\ddagger}$, are lowered by increasing the electronegativity or alternatively the electron affinity of X in each group. A similar trend was noted by Shi and Boyd[3i] for the intrinsic barrier, $\Delta E_0^{\ddagger}$ in the identity exchange reactions involving methyl transfer [R = H in equation (1)]. Inspection of Table 3 indicates that for the allyl transfer reactions an approximate linearity holds between the two types of energy barriers, $\Delta E^{\ddagger}$ and $\Delta E_0^{\ddagger}$, within each group.

Table 4 gives the changes involved in the activation process, i.e. S→TS, in bond distances for $d(C^2–C^3)$ and $d(C^3–X)$ at both the HF and MP2 levels and atomic charges for C^3 and X at the MP2 level. There are systematic changes within each group: the percentage changes ($\Delta d^{\ddagger}/d^0 \times 100$) in $d(C^2–C^3)$ and $d(C^3–X)$ become smaller with increasing electronegativity. This means that within each group or within a row of the Periodic Table, the stronger the electronegativity of X, the smaller is the extent of structural changes involved in the activation process, and the smaller is the activation barrier. This is consistent with the results of Mitchell *et al.*,[15] who defined the percentage change as the distortion index (*DI*) and showed that *DI* reflects 'tightness' or 'looseness' of the TS and $\Delta E_0^{\ddagger}$, for identity methyl transfer increases as *DI* increases or as the electronegativity of X decreases. The intrinsic barriers are found to be linearly correlated with the total deformation energies, which in turn are dominated by the C–X stretching, i.e. *DI*, and are related to the experimental C–X bond dissociation energies.

Again, within each group, the stronger the electronegativity of X, the smaller is the amount of charge transferred to the reaction centre carbon from the

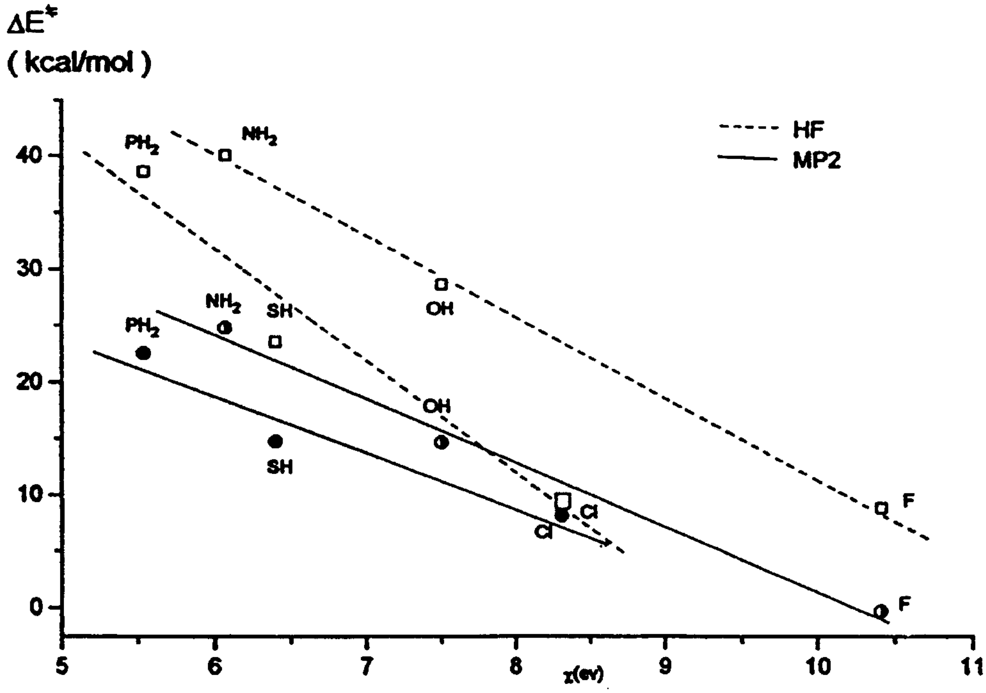

Figure 2. Plots of activation energy ($\Delta E^{\ddagger}$) versus electronegativity (χ)

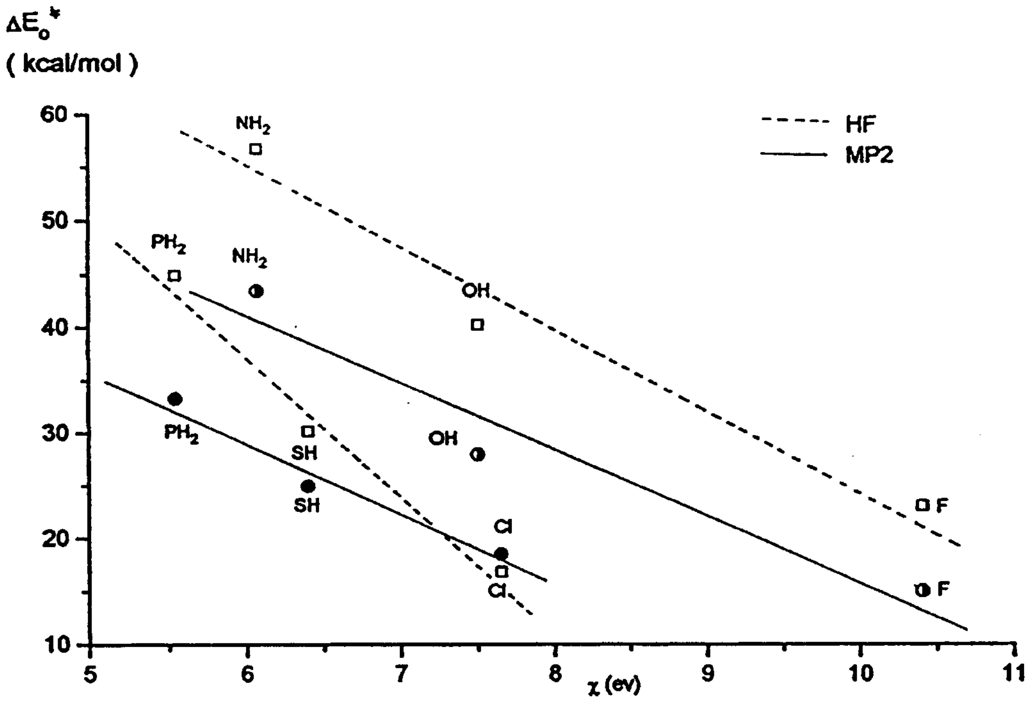

Figure 3. Plots of intrinsic barrier ($\Delta E_0^{\ddagger}$) versus electronegativity (χ)

nucleophile X^- [$\Delta q^{\ddagger}(C^3)$] and to the leaving group X [$\Delta q^{\ddagger}(X)$].

The correlation part of the electronic energy in the S_N2 process is known to change significantly when going along the reaction path from reactants to TS owing to substantial electronic charge redistribution and the formation of a formally penta-coordinated reaction centre carbon atom.[3g] According to the valence bond configuration mixing (VBCM) model of Pross and co-workers,[16a–c] the TS occurs approximately at the crossing point of the reactant (structure **III**) and product VB structures (not shown), and the confidence is affected by contributions from other VB structures, e.g.**IV** and **V**. For a more electronegative X, the contribution of valence bond configuration[3i,16d–f] **IV** to the TS can be greater since a smaller extent of structural and electronic charge reorganization is required.

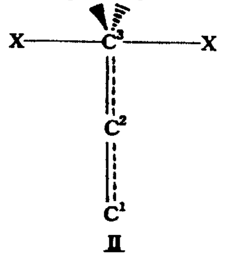

II

$X\cdot$ $\cdot C^3$ $^{-}{:}X$

III

$X{:}^{-}$ $^{+}C^3$ $^{-}{:}X$

IV

$X\cdot$ $^{-}{:}C^3$ $\cdot X$

V

Comparison of energy barriers for X = F and Cl indicates that the electron correlation effect is especially large for X = F. The two barriers, $\Delta E^{\ddagger}$ and $\Delta E_0^{\ddagger}$, are higher for X = F at the HF level, but in contrast they are lower for X = F than for X = Cl at the MP2 level. These reversals in the order of activation barriers for X = F and Cl with lower correlated barriers for X = F are also found for the identity methyl (R = H) transfer reactions (Table 5), which is in agreement with the experimental activation barriers, $\Delta E_0^{\ddagger}$[2g,3g] This trend is mainly due to a great lowering of the correlated barriers for X = F by inclusion of electron correlation; for X = F, $\Delta E_0^{\ddagger}$ and $\Delta E^{\ddagger}$ are lowered by *ca* 8 and 10 kcal mol^{-1}, respectively, whereas for X = Cl, $\Delta E_0^{\ddagger}$ is raised by 2 kcal mol^{-1} and $\Delta E^{\ddagger}$ is lowered by only less than 1 kcal mol^{-1} by inclusion of electron correlation. Similar trends have been reported for the identity methyl[3i] and acetonitrile group[3j] transfers. Table 5 compares the electron correlation effect on the energy barriers for the two identity exchange reactions. It can be seen that in the methyl transfer reactions, energy barriers are lowered for X = F but they are raised for X = Cl by including electron correlation. In contrast, however, the energy barriers are lowered for X = Cl in the acetonitrile group transfer reaction. Hence the effect of electron correlation on the energy barriers depends on the nature of both the R and X groups. One common feature to the methyl and allyl transfer reactions is that the electron correlation effect is

Table 4. Changes (S→TS) in bond length [$\Delta d^{*}(\%) = (\Delta d^{*}/d^{0}) \times 100$] and changes ($\Delta q^{*}$ in electronic units)[a] for reactions $CH_2CHCH_2X + X^-$

	HF		MP2			
X	$\Delta d^{*}(C^2–C^3)$ (%)	$\Delta d^{*}(C^3–X)$ (%)	$\Delta d^{*}(C^2–C^3)$ (%)	$\Delta d^{*}(C^3–X)$ (%)	$\Delta q^{*}(X)$	$\Delta q(C^3)$
H	+1·4	+53·7	−1·4	+44·1	−0·605	−0·611
NH_2	−1·8	+40·1	−2·3	+37·2	−0·468	−0·367
OH	−1·4	+39·0	−1·9	+35·2	−0·394	−0·286
F	−1·1	+34·8	−1·3	+30·4	−0·319	−0·227
PH_2	−2·2	+39·1	−2·6	+33·7	−0·791	−0·486
SH	−2·1	+38·2	−2·1	+31·6	−0·701	−0·385
Cl	−1·5	+38·5	−2·0	+31·5	−0·619	−0·279

Table 5. Electron correlation (EC) effects on energy barriers (kcal mol^{-1}) for identity exchange reactions of $RCH_2X + X^-$ with R = H and CN

		ΔE_0^{*}		ΔE^{*}	
R	X	HF	HF + (EC)	HF	HF + (EC)
H	F	20·0	17·1	7·4 (5·7)	3·8 (−1·0)[b]
	Cl	15·7	18·1	6·3 (6·6)	8·9 (7·7)[b]
CN	Cl	22·1	11·4[c]	5·8	−5·7

[a] Valence-shell double ζ (DZ) with diffuse functions (D) on X and polarization functions (P) on all atoms (DZDP). Electron correlation was accounted for by the CI(SD) approach.[3g]

[b] At the MP2/6–31++G** level for the values in parentheses.[3h]

[c] At the MP2/6–311+G(2d,2p)//MP2/6–31+G(d,p) level.[3j]

stronger for X = F than for Cl. As a result, the correlated energy barriers for F become smaller than those of Cl.

In order to examine the effects of the group R [in equation (1)] and of the electron correlation, relevant results are compared in Table 6 for the identity exchange reactions involving $RCH_2Cl + Cl^-$ with various R. Some interesting effects of the group R (mostly unsaturated) emerge. (1) As the group electronegativity (χ)[13] or electron-withdrawing power (as represented by Taft's polar substituent constants, σ^{*}, in aliphatic systems)[17] of R increases, the activation barrier, ΔE^{*}, at the MP2 level decreases. A few gas-phase experimental rate constants reported[18] which are directly comparable to the results in Table 6 (for R = H, CH_3 and CN) are consistent with the trend in the activation barrier (ΔEFO^{*}_{MP}), except that there is an uncertainty in the reported rate constant for R = CH_3. However, experimental results for soft nucleophiles (X = HS^- and Cl^-) are in good agreement with our results for X = Cl^- with R = H, CH_3, CH_2CH and CN. (2) The HF energy barriers are lower than the MP2 barriers ($\Delta EFO^{*}_{HF} < \Delta EFO^{*}_{MP}$) for substrates with a weakly electronegative R, but this order of energy barrier reverses to $\Delta EFO^{*}_{HF} > \Delta EFO^{*}_{MP}$ for substrates with a strongly electronegative R. (3) The percentage extension of $d(C^3–X)$ in the activation process tends to increase as the electronegativity of R decreases.

Now, if we compare the valence bond configurations **IV** and **V** with the reactant configuration, **III**, **IV** is certainly a more electron-localized structure with a greater hardness and **V** a more delocalized structure with less hardness than **III**.[19] This means that electron correlation is greater in **IV** whereas it is smaller in **V** than in **III**.[19] Hence a greater contribution of structure **IV** to the TS should result in a larger magnitude of electron correlation energy in the TS than in the reactant; in contrast, a greater contribution of structure **V** to the TS will result in a smaller magnitude of electron correlation energy in the TS than in the reactant substrate. The effects will be stronger the greater is the contribution of **IV** and **V** to the TS.

If the electron correlation energy in the TS is greater than that in the ground state (substrate), $\Delta E^{*}_{corr} > 0$, a net reduction of correlated energy barriers, ΔE^{*}_{MP}, will result; $\Delta E^{*}_{MP} = (E^{*}_{SCF} - E^{*}_{corr}) - (E^{0}_{SCF} - E^{0}_{corr}) = \Delta E^{*}_{HF} - \Delta E^{*}_{corr} (< \Delta E^{*}_{HF})$ (Figure 4). As the electronegativity of X^- and/or R increases, the contribution of the ionic valence bond configuration, **IV**, to the TS increases, and leads to the lowering of the correlated energy barriers,

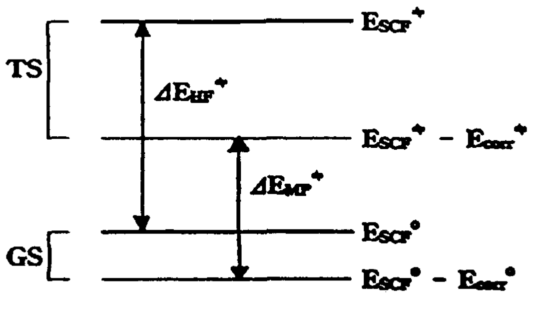

Figure 4. The SCF and correlation energy levels in the ground state (GS) and transition state (TS)

Table 6. Energies (kcal mol^{-1}) calculated at the HF and MP2 levels and changes in bond length [$\Delta d^{\ddagger}(C^3-X)$ in Å] and FMO energy level (in hartree) at the MP2 level for reactions $RCH_2Cl + Cl^-$

	$\Delta E_0^{\ddagger}$		$\Delta E^{\ddagger}$				FMO					
R	HF	MP2	HF	MP2	$d^{\ddagger}(C^3-X)$[a]	$\Delta d^{\ddagger}(C^3-X)$ (%)[b]	π	π^*	σ	σ^*	χ[c]	σ^*[d]
H[e]	15·47	17·34	6·59	7·68	2·316	+30·2					–	0·49
CH_3	18·47	22·20	9·04	11·04	2·361	+32·0					4·42	0·00
$CH_2{=}CH$	16·82	18·80	9·02	8·12	2·360	+31·5(−2·0)	−0·3955	+0·2286	−0·8407	+0·3316	5·18	0·56
$CH{\equiv}C$	20·00	19·06	10·79	6·84	2·343	+30·7(−1·9)	−0·4115	+0·2986	−0·8523	+0·3229	8·21	2·18
$N{\equiv}C$	21·83[f]	17·21[f]	5·70	−0·27	2·294	+29·0(−1·7)	−0·4893	+0·2795	−0·8899	+0·3044	8·63	3·30

[a] Length of the C^3-X bond at the TS.

[b] Percentage change ($S \rightarrow TS$) in $d(C^3-X)$: $(\Delta d^{\ddagger}/d^0) \times 100$. The values in parentheses are the $\Delta d^{\ddagger}(C^3-C^2)$ values.

[c] Electronegativity of the group S.[13]

[d] Taft's polar substituent constant.[17b]

$\Delta E^{\ddagger}_{MP}$, as a result of the increased $E^{\ddagger}_{corr}$ relative to E^{0}_{corr}, i.e., $\Delta E^{\ddagger}_{corr} > 0$.

On the other hand, the HF and MP2 bond distance changes, Δd^{*}, in Table 4 reveal that within each group, the Δd^{*} value is smaller for X with a greater electronegativity; the greater the electronegativity of X, the less is the structural reorganization at both the HF and MP2 levels in the activation process. This is also true for the changes in atomic charges; the electronic reorganization or charge transfer is smaller for the X with a greater electronegativity. We therefore conclude that there are two effects of electronegativity of X and/or R: an increase in electronegativity (i) reduces the electronic and structural reorganizations required in the activation process leading to HF ($\Delta E^{\ddagger}_{HF}$) as well as correlated energy barriers ($\Delta E^{\ddagger}_{MP}$), and (ii) increases the electron correlation energy of the TS lowering the $\Delta E^{\ddagger}_{MP}$ value only.

As we have noted above, the main structural reorganization involved in the activation process for the identity exchange reactions, equation (1), is the extension of C^3–X. The structural changes are determined solely by the requirement to assist charge transfer to the maximum extent.[20] According to the principles of the inter-frontier level gap ($\Delta\mathscr{E}_{FMO} = \mathscr{E}_{LUMO} - \mathscr{E}_{HOMO}$) narrowing and frontier electron density growing of Fukui and Fujimoto,[21] the LUMO, $\sigma^{*}_{(C-X)}$, is lowered and frontier electron density grows as a reaction proceeds along the reaction coordinate until the TS is reached in order to attain the facile charge transfer required in the TS by providing sufficient charge transfer stabilization, E_{ct}; a lower σ^{*}_{LUMO} and a greater frontier electron density lead to a greater charge transfer stabilization energy, E_{ct}, by reducing the inter-frontier level gap, $\Delta\mathscr{E}_{FMO}$, and increasing H_{ij}, respectively, in the equation

$$E_{ct} \approx \frac{H_{ij}^{2}}{\Delta\mathscr{E}_{FMO}} \qquad (2)$$

Therefore, if σ^{*}_{LUMO} is low already in the initial state† (reactant substrate) due to a strong electronegativity of X and/or R, further assistance required to attain the maximum charge transfer by proceeding along the reaction coordinate, i.e., by expanding the C^3–X bond, until the TS is reached can be small, and the TS will be reached by a small extension of C^3–X.

Our HF/6–31++G**//HF/6–31++G** level calculations on **I** and **II** with Nu = X = H reveal that the effects of R = C_6H_5 in **I** is similar to those of R = CH_2CH in **II**; the ΔE^{*} values are 61.22 kcal mol^{-1} for **I** and 63.62 kcal mol^{-1} for **II**, and $d^0(C^{\alpha}-C^1)$ = 1·5117 Å contracts by 1.7% and d^0(C–X) = 1·0859 Å expands by 53.1% in the activation process for **I**, which compare well with the corresponding changes of −1·4% from $d^0(C^3-C^2)$ = 1·5025 Å and +53·7% from d^0(C–X) = 1·0869 Å for **II**. The two R groups in fact have very similar group electronegativities (the χ values reported are 5·20 and 4·85 for C_6H_5 and $CH_2{=}CH$ respectively[14]) and Taft's polar substituent constant, σ^{*} (= 0·60 for R = C_6H_5 and 0·56 for R = CH_2CH).[17b] We therefore think that the allyl system, **II**, can provide a satisfactory model for the benzyl system, **I**.

In this respect, the benzylic effect of structure **I**[4,5] seems to depend on the electronegativity effect of benzene ring and a smaller extent of bond contraction of the C^{α}–C^1 bond is in fact more conducive to a rate enhancement, i.e. a lower activation energy, owing to a lesser extent of structural and electronic reorganization required in the TS. This is in contrast to the common conception that a greater benzylic effect is associated with a greater bond contraction of C^2–C^3 in **II** or C^{α}–C^1 in **I**, leading to a greater lowering of the activation energy.

As a result of the π orbital overlap, electronic charge actually flows out of the R group into the C^3–X bonds [$\pi_{(R)} \rightarrow \alpha^{*}_{(C-X)}$]. If the charge were accepted by the R group [$\sigma_{(C-X)} \rightarrow \pi^{*}_{(R)}$] resonance delocalization of the C^3–X orbitals into the π^{*} orbitals of the R group should result in a greater contraction of the C^3–C^2 bond for a stronger C^3–X bond, i.e. a greater decrease in $\Delta d^{*}(C^3-C^2)$ should result from a smaller increase in $\Delta d^{*}(C^3-X)$, which is contrary to our findings in Tables 4 and 6. This is especially true for the changes in these bond distances with variation of R (Table 6). The electronegativity of R is greater for CH≡C than for $CH_2{=}CH$, so that we would have expected the extent of resonance electron delocalization to be greater in $CH{\equiv}CCH_2Cl$ if the electronic charge were to flow into the R group from the C^3–X orbitals because of the stronger electronegativity of CH≡C. The results (Table 6) are, however, the opposite to this expectation, indicating again that the charge is donated from $\pi_{(R)}$ to $\sigma^{*}_{(C-X)}$. This is supported by the lower inter-frontier level gaps $\Delta\mathscr{E}_1 = \pi_{(R)} - \sigma^{*}_{(C-Cl)}$ than $\Delta\mathscr{E}_2 = \sigma_{(C-Cl)} - \pi^{*}_{(R)}$ (Table 6), since charge-transfer stabilization, E_{ct} [equation (2)], will be favoured by a smaller energy gap, $\Delta\mathscr{E}_1$, i.e. $\pi_{(R)} - \sigma^{*}_{(C-X)}$ interaction.

The activation barriers shown in Table 6 demonstrate that even though the methyl transfer reaction (R = H) does not involve any benzylic effect in the TS, the correlated activation barrier, $\Delta E^{\ddagger}_{MP}$, is lower than that

---

† In line with the well known trend of the lower $\sigma^{*}_{(C-X)}$ LUMO level for a substrate with a more electron-withdrawing (or a more electronegative) substituent (X and/or R), the LUMO [$\sigma^{*}_{(C-X)}$] level is successively lowered as the electronegativity of the X and/or R groups increases. the HF $\sigma^{*}_{(C-X)}$ levels for CH_2CHCH_2X are 0·6188 (X = NH_2), 0·5462 (OH), 0·4633 (F), 0·3822 (PH_2), 0·3649 (SH) and 0·3316 (Cl); for X = Cl, see Table 6.

for the allyl transfer reaction which does involve a benzylic type effect. Steric effects can contribute to the elevation of the activation barrier for the allyl transfer.

Wolfe *et al.*[22] have shown by perturbational molecular orbital (PMO) analyses that the availability of acceptor orbitals on R introduces a stabilizing contribution due to the orbital interactions forming the HOMOs, especiably of type A for TS $(X\text{–}CRH_2\text{–}X)^-$, where the Xs have non-bonding orbitals. The decreasing $\Delta E^{\ddagger}_{\mathrm{MP}}$ values with the increasing acceptor ability as measured by the increasing positive Taft's σ^* constant or by the increasing electronegativity in Table 6 are consistent with the results of such analyses. On the other hand, according to the state correlation diagram (SCD) approach of Shaik *et al.*,[16d,23] the barrier height of an S_N2 process can be given by a fraction (f) of the energy gap between the ionization potential of the nucleophile ($I_{\mathrm{N:}}$) and the electron affinity of the substrate (A_{RX}), $I_{\mathrm{N:}} - A_{\mathrm{RX}}$ less the avoided crossing B. This approach predicts that π-acceptor α-carbon substituents such as CH_2CH, CHCH, CN and C_6H_5 improve the substrate acceptor ability markedly without greater delocalizing the $C^3\text{–}X^-$ bond. Hence these substituents will enhance reactivity towards powerful nucleophiles. Our results for $\Delta E^{\ddagger}_{\mathrm{MP}}$ in Table 6 indeed show lower barriers for α-substitution of CHCH and CN. The small barrier height difference ($\Delta\Delta E^{\ddagger}_{\mathrm{MP}} = 0{\cdot}44\ \mathrm{kcal\,mol^{-1}}$) obtained for substitution of CH_2CH has been ascribed to the opposing effects on f and the energy gap brought about by the α-vinyl group. A similar explanation has been advanced by Shaik *et al.* for the small reactivity difference due to α-phenyl substitution.

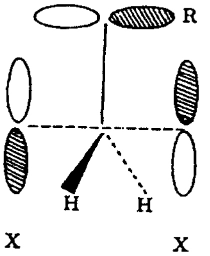

A

In these two approaches, PMO and SCD, the increased in acceptor ability arising from the α-substitution of R plays an important role in the rate enhancement observed.

SUPPLEMENTARY MATERIALS

Detailed geometries of all structures and energies studied are available.

ACKNOWLEDGEMENTS

We thank the Korea Research Centre for Theoretical Physics and Chemistry for support of this work. One of us (C.K.K.) also thanks Inha University for a Postdoctoral Fellowship. We are indebted to Professor R. J. Boyd for providing us with the results of the identity methyl transfer reactions.

REFERENCES

1. I. Lee, N. D. Kim and C. K. Kim, *J. Phys. Org. Chem.* **6**, 499 (1993).
2. (a) W. N. Olmstead and J. I. Brauman, *J. Am. Chem. Soc.* **99**, 4219 (1977); (b) M. J. Pellerite and J. I. Brauman, *J. Am. Chem. Soc.* **102**, 5993 (1980); (c) M. J. Pellerite and J. I. Brauman, *J. Am. Chem. Soc.* **105**, 2672 (1983); (d) C. C. Han and J. A. Dodd, *J. Phys. Chem.* **90**, 471 (1986); (e) J. A. Dodd and J. I. Brauman, *J. Phys. Chem.* **90**, 3559 (1986); (f) K. Tanaka, G. I. Mackay, J. D. Payzant and D. K. Bohme, *Can. J. Chem.* **54**, 1643 (1976); (g) S. E. Barlow, J. M. Van Doren and V. M. Bierbaum, *J. Am. Chem. Soc.* **110**, 7240 (1988).
3. (a) D. J. Mitchell, PhD Thesis, Queens University, Kingston, Ont. (1981); (b) S. Wolfe, D. J. Mitchell and H. B. Schlegel, *J. Am. Chem. Soc.* **103**, 7672, 7674 (1981); (c) S. S. Shaik, H. B. Schlegel and S. Wolfe, *Theoretical Aspects of Physical Organic Chemistry*, Chapt. 5. Wiley, New York (1992); (d) F. Carrion and M. J. S. Dewar, *J. Am. Chem. Soc.* **106**, 3531 (1984); (e) P. Sand, J. Bergman and E. Lindholm, *J. Phys. Chem.* **92**, 2039 (1988); (f) S. C. Tucker and D. G. Truhlar, *J. Am. Chem. Soc.* **112**, 3338, 3347 (1990); (g) R. Vetter and L. Zülicke, *J. Am. Chem. Soc.* **112**, 5136 (1990); (h) Z. Shi and R. J. Boyd, *J. Am. Chem. Soc.* **112**, 6789 (1990); (i) Z. Shi and R. J. Boyd, *J. Am. Chem. Soc.* **113**, 2434 (1991); (j) B. D. Wladkowski, K. F. Lim, W. D. Allen and J. I. Brauman, *J. Am. Chem. Soc.* **114**, 9136 (1992).
4. (a) R. A. Marcus, *J. Chem. Phys.* **26**, 867, 872 (1957); (b) R. A. Marcus, *J. Phys. Chem.* **72**, 891 (1968).
5. (a) J. F. King and G. T. Y. Tsang, *J. Chem. Soc., Chem. Commun.* 1131 (1979); (b) J. I. Lynas and C. J. M. Stirling, *J. Chem. Soc., Chem. Commun.* 483 (1984); (c) D. Kost and K. Aviram, *J. Am. Chem. Soc.* **108**, 2006 (1986); (d) T. L. Amyes and W. P. Jencks, *J. Am. Chem. Soc.* **111**, 7900 (1989).
6. I. Lee, J. K. Cho and C. K. Kim, *Bull. Korean Chem. Soc.* **12**, 182 (1991).
7. W. J. Hehre, L. Radom and P. v. R. Schleyer and J. A. Pople, *Ab Initio Molecular Orbital Theory.* Wiley, New York (1986).
8. (a) J. A. Pople, R. Krishnan, H. B. Schlegel and J. S. Binkley, *Int. J. Quantum Chem.* **S13**, 225(1979); (b) J. A. Pople, H. B. Schlegel, R. Krishnan, D. J. DeFrees, J. S. Binkley, M. J. Frisch, R. A. Whiteside, R. F. Hout and W. J. Hehre, *Int. J. Quantum Chem.* **S15**, 269 (1980).
9. Y.-D. Wu and K. N. Houk, *J. Am. Chem. Soc.* **109**, 906 (1987); especially see footnote 7.
10. (a) A. E. Reed, L. A. Curtiss and F. Weinhold, *Chem. Rev.* **169**, 41 (1988); (b) F. Weinhold and J. E. Carpenter, *The Structure of Small Molecules and Ions*, p. 227. Plenum Press, New York (1988).
11. M. J. Frisch, G. W. Trucks, M. Head-Gordon, P. M. W. Gill, M. W. Wong, J. B. Foresman, B. G. Johnson, H. B. Schlegel, M. A. Robb, E. S. Replogle, R. Gomperts, J. L. Andres, K. Raghavachari, J. S. Binkley, C. Gonzalez, R.

L. Martin, D. J. Fox, D. J. DeFrees, J. Baker, J. J. P. Stewart and J. A. Pople, *Gaussian 92, Revision C*. Gaussian, Pittsburgh, PA (1992).

12. R. T. Sanderson, *Chemical Bond and Bond Energy*, p. 12. Academic Press, New York (1971).
13. F. De Proft, W. Langenaeker and P. Geerlings, *J. Phys. Chem.* **97**, 1826 (1993).
14. R. G. Pearson, *J. Org. Chem.* **54**, 1423 (1989).
15. D. J. Mitchell, H. B. Schlegel, S. S. Shaik and S. Wolfe, *Can. J. Chem.* **63**, 1642 (1985).
16. (a) A. Pross and S. S. Shaik, *J. Am. Chem. Soc.* **104**, 187 (1982); (b) A. Pross and S. S. Shaik, *Acc. Chem. Res.* **16**, 363 (1983); (c) D. J. McLennan and A. Pross, *J. Chem. Soc., Perkin Trans. 2* 981 (1984); (d) S. S. Shaik, *Prog. Phys. Org. Chem.* **15**, 197 (1985); (e) A. Pross and S. S. Shaik, *J. Am. Chem. Soc.* **103**, 3702 (1981); (f) A. Pross, *Adv. Phys. Org. Chem.* **21**, 99 (1985).
17. (a) R. W. Taft, *J. Am. Chem. Soc.* **74**, 3120 (1952); (b) J. A. Dean, *Handbook of Organic Chemistry*, Table 7-1. McGraw-Hill, New York (1987).
18. C. H. Depuy, S. Gronert, A. Mullin and V. M. Bierbaum, *J. Am. Chem. Soc.* **112**, 8650 (1990).
19. R. G. Pearson, *J. Org. Chem.* **54**, 1423 (1989).
20. M. Godfrey, *J. Chem. Soc., Perkin Trans. 2* 139 (1988).
21. (a) K. Fukui and H. Fujimoto, *Bull. Chem. Soc. Jpn* **42**, 3399 (1969); (b) K. Fukui, *Theory of Orientation and Stereoselection*. Springer, Berlin (1975).
22. S. Wolfe, D. J. Mitchell and H. B. Schlegel, *Can. J. Chem.* **60**, 1291 (1992).
23. (a) S. S. Shaik, H. B. Schlegel and S. Wolfe, *Theoretical Aspects of Physical Organic Chemistry. The S_N2 Mechanism*, p. 122. Wiley, New York (1992); (b) S. S. Shaik, *J. Am. Chem. Soc.* **105**, 4359 (1983).